NeuroImage 56 (2011) 1546–1555

Contents lists available at ScienceDirect

NeuroImage

journal homepage: www.elsevier.com/locate/ynimg

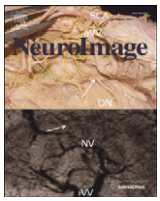

Resting-state networks in the macaque at 7 T☆

R. Matthew Hutchison [a,b,d], L. Stan Leung [a,b], Seyed M. Mirsattari [a,c,d], Joseph S. Gati [d], Ravi S. Menon [a,d], Stefan Everling [a,b,d,*]

[a] Graduate Program in Neuroscience, University of Western Ontario, London, Ontario, Canada
[b] Department of Physiology and Pharmacology, University of Western Ontario, London, Ontario, Canada
[c] Department of Clinical Neurological Sciences, University of Western Ontario, London, Ontario, Canada
[d] Robarts Research Institute, London, Ontario, Canada

ARTICLE INFO

Article history:
Received 28 October 2010
Revised 18 February 2011
Accepted 21 February 2011
Available online 26 February 2011

Keywords:
Functional connectivity
Macaque
Resting-state
Independent component analysis (ICA)
Spontaneous activity
Functional MRI (fMRI)

ABSTRACT

Assessment of brain connectivity has revealed that the structure and dynamics of large-scale network organization are altered in multiple disease states suggesting their use as diagnostic or prognostic indicators. Further investigation into the underlying mechanisms, organization, and alteration of large-scale brain networks requires a homologous animal model that would allow neurophysiological recordings and experimental manipulations. The current study presents a comprehensive assessment of macaque resting-state networks based on evaluation of intrinsic low-frequency fluctuations of the blood oxygen-level-dependent signal using group independent component analysis. Networks were found underlying multiple levels of sensory, motor, and cognitive processing. The results demonstrate that macaques share remarkable homologous network organization with humans, thereby providing strong support for their use as an animal model in the study of normal and abnormal brain connectivity as well as aiding the interpretation of electrophysiological recordings within the context of large-scale brain networks.

Introduction

The mammalian brain is composed of functional networks operating at different spatial and temporal scales — characterized by patterns of interconnections linking sensory, motor, and cognitive systems (Felleman and Van Essen, 1991; Young, 1993; Friston, 2002). Neuroimaging has afforded unparalleled access in the exploration of the topology of these systems, and has revealed that neural processing relies on the dynamic integration of cortical and subcortical areas within large-scale and distributed brain networks (Sporns et al., 2005; Guye et al., 2008). Network activity is typically assessed using functional connectivity measures. This is an examination of temporal correlations that exist between distinct brain areas (Friston, 1994) connected directly or indirectly by long-range cortical and subcortical polysynaptic pathways (Hagmann et al., 2008). Using this definition, functional connectivity has been derived using spontaneous blood oxygenation-level-dependent (BOLD) fluctuations measured by functional magnetic resonance imaging (fMRI; Biswal et al., 1995). Correlation of low frequency fluctuations (LFFs; 0.01–0.1 Hz) of the BOLD signal acquired in the absence of a task has been shown to reflect anatomical connectivity (Vincent et al., 2007; Honey et al., 2009; Greicius et al., 2009) and presumed to be a hemodynamic manifestation of functional connectivity between slow fluctuations in neuronal activity (Fox and Raichle, 2007; Shmuel and Leopold, 2008).

Investigations of functional connectivity through the evaluation of LFF synchrony during rest have demonstrated that the human brain is spatially organized into coherent patterns characterized as networks. These robust and reproducible resting-state networks (RSNs) have been reported for visual, motor, auditory, language, memory, executive, and attention systems, as well as the default-mode network (Cordes et al., 2000; Raichle et al., 2001; Hampson et al., 2002; Beckmann et al., 2005; Damoiseaux et al., 2006). RSNs parallel previously identified task-based networks and spatio-temporal network synchronization is preserved during sedation and anesthesia in humans, monkeys, and rats (Kiviniemi et al., 2005; Vincent et al., 2007; Hutchison et al., 2010). RSNs can be identified through a seed-region analysis in which spatial functional connectivity maps are inferred by a cross-correlation analysis of the voxel-wise fMRI recordings against a reference time-course. The shortcoming of this technique is that it tests a specific hypothesis and is limited to those areas that are selected as seed-regions (Cole et al., 2010). Owing to the constraints of seed-region analysis, exploratory techniques such as independent component analysis (ICA) are now frequently applied to human functional data sets, where they have revealed RSNs that had not been previously shown with seed-region techniques (Beckmann et al., 2005; Smith et al., 2009).

☆ Grant sponsor: Canadian Institutes of Health Research (CIHR).
* Corresponding author at: The Centre for Brain and Mind, Robarts Research Institute, 100 Perth Drive, London, Ontario, Canada N6A 5K8. Fax: +1 519 931 5233.
E-mail address: severlin@uwo.ca (S. Everling).

1053-8119/$ – see front matter © 2011 Elsevier Inc. All rights reserved.
doi:10.1016/j.neuroimage.2011.02.063

Although their meaning is not fully understood, changes in functional RSNs have been recently reported in several psychiatric and developmental disorders including depression, attention deficit-hyperactivity disorder, schizophrenia, Alzheimer's disease, epilepsy, and multiple sclerosis (Auer, 2008; Greicius, 2008). Given the extraordinary potential for RSNs as possible diagnostic or prognostic markers, it is crucial to understand the physiological mechanisms of fluctuation, regulation, and entrainment of LFFs and the RSNs that are revealed through their synchronization.

Nonhuman primates and in particular macaque monkeys have been used as surrogates for the study of human brain function for several decades and might therefore represent an ideal animal model for the study of RSNs. Although macaque and human brains share a high degree of similarity in terms of cytoarchitecture (Petrides and Pandya, 1999, 2002a; Ongür et al., 2003), functional organization (Rees et al., 2000; Koyama et al., 2004; Petrides et al., 2005; Nakahara et al., 2007), and anatomical connections (Croxson et al., 2005; Kelly et al., 2010), there also exist structural (Preuss, 2000; Rilling, 2006), morphological (Buxhoeveden et al., 2001), and functional (Orban et al., 2004; Preuss, 2004) differences between the brains of these two primate species (Passingham, 2009).

While a few recent studies have revealed homologous RSNs between human and nonhuman primates, these studies either utilized seed-region analysis (Vincent et al., 2007, 2010; Margulies et al., 2009) or ICA in only two animals (Moeller et al., 2009). Here, we present a comprehensive evaluation of macaque RSNs at 7 T using group ICA and an analysis methodology that is very similar to what has been used in humans. The results show striking similarity of macaque RSNs to previously described human RSNs.

Material and methods

Animal preparation

Data was obtained from 6 macaque monkeys (*Macaca fascicularis*; 2 male, 4 female) whose weights ranged from 3.6 kg to 5.3 kg (mean +/− SD = 4.58 +/− 1.4 kg). Surgical and experimental procedures were carried out in accordance with the Canadian Council of Animal Care policy on the use of laboratory animals and approved by the Animal Use Subcommittee of the University of Western Ontario Council on Animal Care.

Animals were initially prepared for imaging by undergoing a surgical procedure to place an MRI-compatible, custom-built acrylic head post that served to restrain the head during image acquisition. The post was anchored to the skull with 6 mm ceramic bone screws (Thomas Recording, Giessen, Germany) and dental acrylic.

On the day of scanning, anesthesia was first induced by intramuscular injections of atropine (0.4 mg/kg), ipratropium (0.025 mg/kg), and ketamine hydrochloride (7.5 mg/kg). Animals were then administered 3 ml of propofol (10 mg/ml) intravenously via the saphenous vein. Following oral intubation with an endotracheal tube, anesthesia was maintained using 1.5% isoflurane mixed with oxygen. Animals were spontaneously breathing throughout the duration of the experiment. The animal was placed in a custom-built primate chair containing fixation for head immobilization and an integrated custom RF coil, and inserted into the bore for image acquisition. The isoflurane level was then lowered to 1% for imaging experiments. Rectal temperature via a fiber-optic temperature probe (FISO, Quebec City, QC), respiration via bellows (Siemens Corp., Union, NJ), and end-tidal CO_2 via capnometer (Covidien-Nellcor, Boulder, CO) were continuously monitored. Physiological parameters were in the normal range (temperature: 36.5 °C; breathing: 25–30 breaths/min; end-tidal CO_2: 24–28 mm Hg) throughout the duration of the experiment. Warmth was maintained using a heating disk (Snugglesafe, Littlehampton, West Sussex, UK) and thermal insulation.

Anesthesia was utilized in this study to eliminate motion effects, physiological stress, and training requirements. Although isoflurane has been shown to have vasodilator properties (Farber et al., 1997) altering cerebrovascular activity in a dose-dependent manner (Vincent et al., 2007), synchronous spontaneous BOLD fluctuations have been previously reported using an isoflurane regime in both monkeys (Vincent et al., 2007) and rats (Hutchison et al., 2010). However, it is still likely that anesthesia can affect RSNs.

Data acquisition

All data were acquired on an actively shielded 7 Tesla 68 cm horizontal bore human head scanner with a DirectDrive console (Varian, Yarnton, UK; Walnut Creek, CA) and a Siemens AC84 gradient subsystem (Erlangen, Germany) operating at a slew rate of 350 mT/m/s. An in-house designed and manufactured conformal 5 channel transceive primate head RF coil was used for all experiments. Magnetic field optimization (B_0 shimming) was performed using an automated, three-dimensional mapping procedure over the specific imaging volume of interest. For each monkey, 2 runs of 300 continuous EPI functional volumes (TR = 2000 ms; TE = 16 ms; flip angle = 70°, slices = 30, matrix = 72 × 72; FOV = 96 × 96 mm; acquisition voxel size = 1.3 × 1.3 × 1.5 mm) were acquired. The total acquisition time of each scan was 10 min. EPI images were acquired with GRAPPA at an acceleration factor of 2. Every image was corrected for physiological fluctuations using navigator-echo-correction. A high-resolution T2-weighted anatomical reference volume was acquired along the same orientation as the functional images using a fast spin echo acquisition scheme (TR = 5000 ms; TE = 38.6 ms; echo train length = 5, effective echo = 3, slices = 30, matrix = 256 × 250; FOV = 96 × 96 mm; acquisition voxel size = 375 μm × 384 μm × 1.5 mm). T2 imaging using fast spin echo, as compared to gradient echo based imaging such as T1-weighted MP-RAGE, reduced the amount of image distortion caused by skull implants such as the ceramic bone screws and plastic head post.

Image preprocessing

All preprocessing was implemented using the FSL software package (http://www.fmrib.ox.ac.uk.) and included motion correction (six parameter affine transformation), brain extraction, spatial smoothing (FWHM = 3 mm), high-pass temporal filtering (Gaussian-weighted least-squares straight line fitting with sigma = 100 s), low-pass temporal filtering (HWHM = 2.8 s, Gaussian filter), and normalization (12 DOF linear affine transformation implemented in FLIRT) to the F99 atlas template (Van Essen, 2004; see http://sumsdb.wustl.edu/sums/macaquemore.do).

Group independent component analysis

Group ICA, unlike single-subject, ICA allows inferences to be made at the group level. When examining subjects individually, it is difficult to compare components since they are not ordered and different components may be revealed in each subject. Entering all subjects into an ICA analysis and estimating one set of components has the advantage of ordering the components of different subjects in the same way. This produces a single set of "group" components that can then be interpreted. Additionally, weak sources with different characteristics across subjects (i.e., noise) will be suppressed allowing a more accurate reflection of population dynamics.

Group ICA was conducted using the GIFT software package (Calhoun et al., 2001; http://icatb.sourceforge.net). Data from both runs of all animals were concatenated, and the temporal dimension of this aggregated data set was reduced by means of principal component analysis (PCA). This was followed by spatial component estimation using the Infomax algorithm. Component time-courses and spatial maps for each animal were then back-reconstructed, using

the aggregated components and the results from the data reduction step (Jafri et al., 2008; Calhoun et al., 2001). Because ICA is a stochastic estimation process, the final component maps can vary depending on the initial algorithm conditions. To quantify the reliability of the decomposition, ICA was reiterated 20 times using the ICASSO toolbox (Himberg et al., 2004). ICASSO represents each of the estimated components for each iteration as a point in the signal space. It then returns a stability index of the estimate cluster computed as the difference between the average intra- and inter-cluster similarities. In the ideal case, the repeated estimates are concentrated in compact and close-to-orthogonal clusters resulting in an index of all estimate-clusters that approaches one.

There are currently no well-established criteria to guide the selection of an optimal number of independent components (ICs) for a given data set (Cole et al., 2010). The model order or dimension estimate defines the number of components that the algorithm will extract and in that regard represents a prediction about the number of underlying sources in the data. If the model order is increased, a greater number of networks will be found accounting for the data in a more detailed way, albeit causing networks to branch into smaller sub-networks (Smith et al., 2009; Abou-Elseoud et al., 2010). One proposed method uses the minimum description length criterion for dimension estimation (Jafri et al., 2008; Li et al., 2007); however when applied to our data set, this technique resulted in an estimation of 253 ICs. Instead, 20 components were chosen, as this gave a manageable number of components and approximated model orders commonly used in human studies large-scale brain networks (Smith et al., 2009; Abou-Elseoud et al., 2010; Calhoun et al., 2001; Demirci et al., 2009).

The mean group ICs were then scaled to empirically derived z-scores by dividing by the standard deviation of the original time-course. The z-scores approximate the temporal correlation between each voxel and the associated component where the magnitude of the z-score specifies the strength of the linear relationship. A negative z-score indicates voxels in which the BOLD signals are modulated opposite to that of the IC time-course. A z-score value of $+/-1$ was used as the lower limit threshold of functional connectivity.

RSN identification and visualization

The ICA derived components were visually inspected and labeled based on the activation patterns in reference to known anatomical and functional locations. Classification of the components in terms of RSNs was performed by comparison with known macaque functional networks and previously identified RSNs from ICA studies in humans (Beckmann et al., 2005; Damoiseaux et al., 2006; Smith et al., 2009). In addition to identifying spatially independent networks, ICA is able to parse out noise due to physiological fluctuations, motion, and hardware artifacts from the original source data (Thomas et al., 2002; Liao et al., 2006; Perlbarg et al., 2007). Components with high spatial correspondence to cerebrospinal spinal fluid (see Supplementary Fig. 1) or with low correlation to gray matter, were discarded.

Group data were projected from volume data to the F99 cortical surface using the CARET (http://www.nitrc.org/projects/caret) enclosed-voxel method.

Single-subject ICA

Single-subject ICA is better suited to reveal individual features of resting-state connectivity as subtle differences between subjects may get lost in an ICA of a group data set. To examine individual subject maps and allow comparison with a previously published report (Moeller et al., 2009), single subject-ICA was conducted using the same parameters as the group-ICA. The unthresholded group-ICA derived networks were then used as templates to order the component maps from the individual ICA by calculating the spatial correlation coefficient of the unthresholded individual maps.

Functional network connectivity

Spatial ICA maximizes the statistical independence in the spatial domain, though the components are not temporally constrained and ICs can exhibit considerable temporal correlations (Calhoun et al., 2003). The temporal dependencies are significant, albeit not as high as those between regions within an IC (Jafri et al., 2008). Functional network connectivity (FNC) analysis examines these temporal dependencies among ICs to establish the functional connectivity among the large scale networks and has been shown to provide additional information regarding macroscopic brain organization (Jafri et al., 2008; Demirci et al., 2009). FNC analysis was conducted using the FNC software package (http://mialab.mrn.org/software/) using analysis steps described previously (Jafri et al., 2008). One-sample Student's t-tests were used to test statistically significant maximal lagged correlation ($+/-3$ s) combinations from the 55 possible combinations ($p<0.05$, corrected for multiple comparisons).

Results

Resting-state networks

Group-ICA successfully decomposed the resting-state functional data of 6 monkeys into 20 independent components. ICASSO returned a stability index for each estimate-cluster that approached 1 (mean $+/-$ SD $= 0.980 +/- 0.006$), indicating that the components are concentrated in compact and close-to-orthogonal clusters and highly consistent across multiple ICA runs. Eleven components were found to have a high correspondence with gray matter as well as showing network characteristics (i.e. spatial maps containing more than one functional area) and were thereby deemed to be physiologically relevant. The spatial maps of the RSNs obtained with ICA analysis are illustrated in Fig. 1 (for RSN maps displayed on a flattened cortex see Supplementary Fig. 2). The components accounted for 59.81% of the data's variance. The degree of cortical coverage is illustrated in Supplementary Fig. 3. Despite inclusion of the entire brain, components were primarily restricted to cortical areas. Therefore we focus on cortical connectivity in this study. On the basis of our classification results, the 11 RSNs can be described as follows:

- *RSN A* (*precentral–temporal*): The RSN included extended bilateral areas of the ventral precentral gyrus, corresponding to ventral premotor areas F4 and F5, activation in the inferior ramus of the arcuate sulcus, the precentral opercular cortex, primary and secondary somatosensory cortex, and insular cortex. In addition, connectivity was observed with the auditory cortex. The network included areas that correspond to the ventral motor system thought to play an important role in understanding action and visuomotor control of grasping and also included areas underlying the control of mouth and tongue (Nelissen et al., 2005; Joly et al., 2009; Phillips and Porter, 1977).
- *RSN B* (*fronto-parietal*): Bilateral connectivity was found in the anterior bank, fundus, and posterior bank of the inferior arm of the arcuate sulcus. The anterior extent of this region corresponds to the location of the frontal eye fields (Bruce and Goldberg, 1985). Connectivity was found in the ventral prefrontal cortex and dorsal premotor cortex. Further network connectivity was found in area 3B in the dorsal central sulcus fundus and in both banks of the intraparietal sulcus. In addition, the right hemisphere showed positive correlation of area 6, corresponding to the supplementary motor area or possibly the supplementary eye fields (Schlag and Schlag-Rey, 1987). The network includes brain areas associated with the oculomotor system (also referred to as the dorsal attention network) responsible for goal-oriented saccadic eye movements (Johnston and Everling, 2008) and mediating goal-directed top-down processing (Noudoost et al., 2010). The functional network

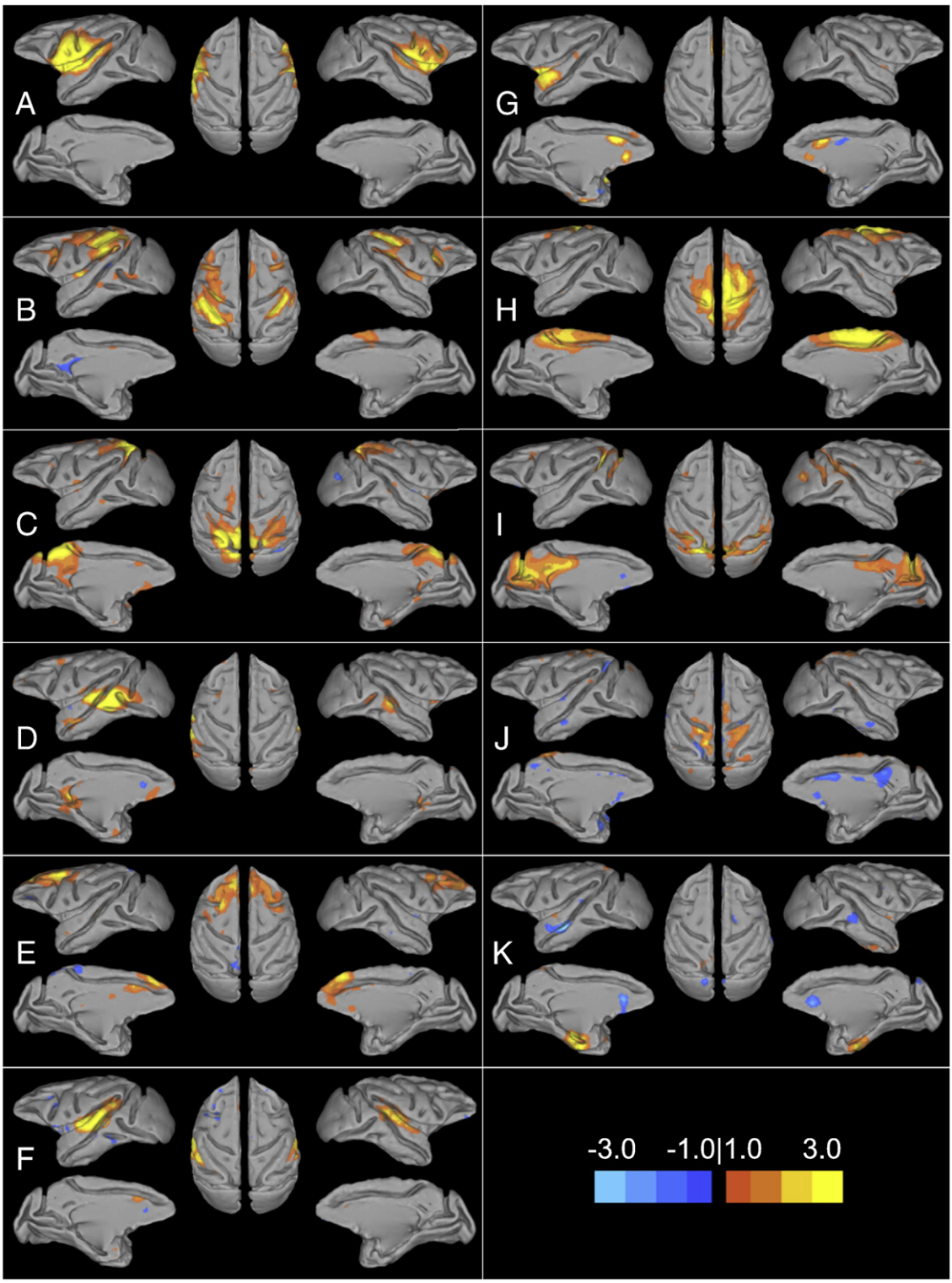

Fig. 1. Cortical representation of eleven resting-state networks (RSNs) identified by independent component analysis of fMRI data acquired from isoflurane-anesthetized macaque monkeys (N = 6). Overlaid color maps represent thresholded z-scores. All images have been normalized to the space of the F99 template (Van Essen, 2004; see http://sumsdb.wustl.edu/sums/macaquemore.do). For each RSN, the left images depict lateral and medial views of left hemisphere, the center images depict the dorsal view of both hemispheres, and the right images depict the lateral and medial views of right hemisphere. Potential functional roles of each network are discussed in the text.

has been previously reported in eye movement tasks (Baker et al., 2006; Ford et al., 2009) and resting-state analysis (Vincent et al., 2007) of the macaque.

- *RSN C* (*posterior-parietal*): The network encompassed the posterior cingulate/precuneus cortex, bilateral areas PG and PE of the parietal cortex, and visual areas V2 and V3. In addition, this network contained connectivity patterns in the dorsolateral prefrontal cortex and in the dorsal premotor cortex in the left hemisphere. The brain areas include areas found in the default-mode network (DMN) areas that are deactivated during attention-demanding cognitive tasks

and in humans has been suggested to support higher-order mental faculties (Raichle et al., 2001).

- *RSN D* (*occipito-temporal*): Network areas included bilateral area TO, V4, TEO, and the arcuate sulcus. Bilateral area 29 and Brodmann area 10 (left hemisphere) were also functionally connected. Previous studies have shown these temporal lobe areas are critical for higher-order visual processing (Tsao et al., 2003).
- *RSN E* (*frontal*): This RSN encompassed bilateral regions in several prefrontal areas, including the anterior bank of the arcuate sulcus, corresponding to the frontal eye fields, the upper ramus of the arcuate sulcus, the posterior portion of the principal sulcus, as well as the dorsal bank of the principal sulcus. In addition, LFF synchronization was also found in area 9, the premotor cortex and the anterior cingulate cortex. These frontal/prefrontal areas have been shown to be components of the executive system suggested to provide bias signals to other areas of the brain in order to implement cognitive control (Miller and Cohen, 2001).
- *RSN F* (*superior-temporal*): A network encompassing the auditory belt, parabelt, and bilateral area 22 on the superior temporal gyrus. Anti-correlated areas were found in the left principal sulcus and in the left arcuate sulcus. The network pattern resembles the mean functional activity resulting from the presentation of multiple sounds categories in a previous task-based fMRI study of the awake monkey (Petkov et al., 2008) and is likely responsible for acoustic processing and interpretation (Rauschecker and Scott, 2009).
- *RSN G* (*cingulo-insular*): A network of areas including bilateral regions in the insular cortex, the anterior cingulate cortex area 24a/b, and the orbitofrontal cortex, area 14. These areas have been associated with the reward system involved in the regulation and control of behavior (Kringelbach, 2005).
- *RSN H* (*paracentral*): A network reflective of the dorsal motor system involved in the control of limb movements (Dum and Strick, 2002). Network connectivity included bilateral primary motor cortex dorsally and also in the central sulcus, area F2, and the dorsal bank of the superior ramus of the arcuate sulcus. In addition, widespread connectivity was found in the medial wall, including the cingulate motor area, supplementary motor area, and medial parietal cortex. The network pattern closely resembles the "somatomotor" network previously described in the anesthetized macaque using a seed-region based approach (Vincent et al., 2007).
- *RSN I* (*parieto-occipital*): A network consisting of regions involved in visual processing including bilateral areas V1, V2, V2, V3, area PO, and area MT/MST. Connectivity was also observed unilaterally in area 8A (left hemisphere) and 46d (right hemisphere). Similar network patterns have been observed in the macaque in both resting-state (Vincent et al., 2007) and awake fMRI studies (Stefanacci et al., 1998).
- *RSN J* (*postcentral*): A network including the postcentral and precentral gyrus, areas dedicated to somatosensory processing (Kaas, 1993). Opposite modulation was found to occur in area PO and in the anterior cingulate cortex area 24 a/b.
- *RSN K* (*hippocampal*): A medial temporal network corresponding to areas associated with the macaque declarative memory system (Squire and Zola-Morgan, 1991). The RSN bilaterally encompassed the hippocampus, entorhinal, perirhinal, and parahippocampal cortical areas. Anti-correlated bilateral connectivity of anterior cingulate cortex area 25 was also observed. The network, although partially explored in several previous electrophysiological studies (e.g. Rolls et al., 1993; Wirth et al., 2003) has not been shown with monkey fMRI possibly due to the difficult task demands required of the animals in order to elicit activations in these areas.

Single subject ICA

To compare single subject ICA with group ICA components, we spatially correlated unthresholded single subject IC maps with the unthresholded group IC maps. The correlation coefficients for all maps and all animals was significant ($p<10^{-20}$, p value corrected for multiple comparisons using Bonferroni correction). Table 1 shows the mean correlation coefficients between the single-subject ICA components and the group-ICA networks. Mean correlation values were found to be significantly different from 0 (one sample t-test, $p<0.01$). A representative network (RSN B — fronto-parietal) is shown for all monkeys in Fig. 2. Networks for all animals are shown in Supplementary Figs. 4–9. In some animals, the same single subject component was best correlated to two or more of the group ICA networks (for example, Supplementary Fig. 5: components corresponding to networks D and I are the same).

Functional network connectivity

Fig. 3 shows a FNC diagram for the 11 identified RSNs. RSNs are represented by circular nodes and significantly correlated RSNs are represented by connecting lines. For example, a line connects networks I and J, representing significant functional connectivity between those two networks. RSN C (posterior-parietal) and RSN I (parieto-occipital) represent the most connected nodes. RSN D (occipito-temporal) and RSN E (frontal) also show a high degree of FNC. The other sensory networks show little or no connectivity with other RSNs.

Discussion

Alterations in functional connectivity recorded using spontaneous BOLD fluctuations have been suggested as the origin or product of multiple disease states (Auer, 2008; Greicius, 2008). Assessing their electrophysiological correlate(s) and establishing the relationship between large-scale functional network connectivity and disease require a suitable animal model. Here, to the best of our knowledge, we report the first comprehensive application of group independent component analysis (ICA) to monkey fMRI data and the first resting-state examination of the macaque at 7 T. ICA successfully identified 11 prominent macaque RSNs representing multiple levels of neural processing. Networks encompassing sensory and motor areas, including the visual, auditory, motor, and somato-sensory regions, can be considered to be lower-order in a cognitive processing hierarchy. The RSNs comprising areas known to be involved in executive control, attention, reward evaluation, and default-mode activity may represent higher-order processing, with temporal networks putatively responsible for visual processing and memory providing intermediate processing. In cases where the system has been explored with fMRI, the patterns of intrinsic functional connectivity are consistent with stimulus-evoked patterns found in task-based studies (see Results). The functional RSNs reported in the

Table 1
Spatial correlations of single subject ICA derived networks to group-ICA derived networks.

Network	Mean	STD ERR	Range
A	0.691	0.068	0.383–0.841
B	0.560	0.082	0.176–0.750
C	0.463	0.062	0.227–0.649
D	0.501	0.078	0.215–0.743
E	0.373	0.046	0.275–0.584
F	0.459	0.073	0.184–0.623
G	0.372	0.060	0.200–0.586
H	0.559	0.059	0.272–0.661
I	0.501	0.065	0.199–0.655
J	0.375	0.045	0.207–0.546
K	0.264	0.017	0.186–0.302

Note: Mean correlation values are significantly different from 0 (one sample t-test, $p<0.01$).

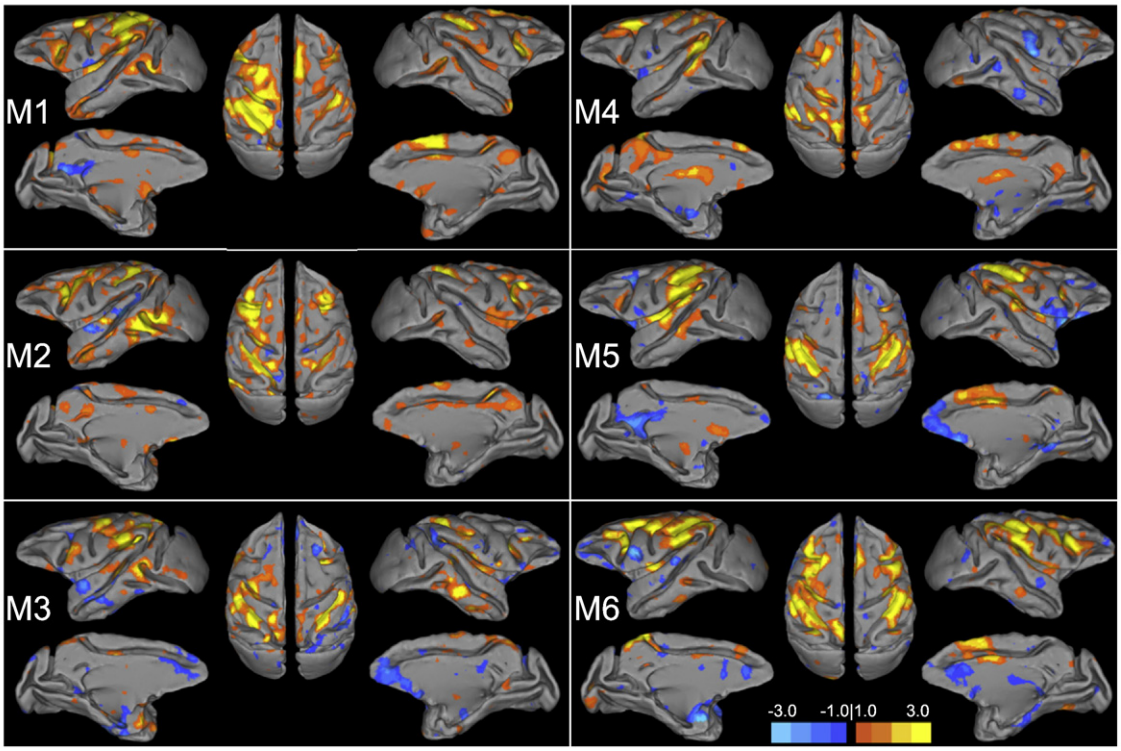

Fig. 2. Resting-state networks (RSN) of all monkeys (M1–M6) following single-subject independent component analysis (ICA) that were most spatially correlated to group-ICA identified RSN B (fronto-parietal). Overlaid color maps represent thresholded z-scores. All images have been normalized to the space of the F99 template (Van Essen, 2004; see http://sumsdb.wustl.edu/sums/macaquemore.do). For each RSN, the left images depict lateral and medial views of left hemisphere, the center images depict the dorsal view of both hemispheres, and the right images depict the lateral and medial views of right hemisphere.

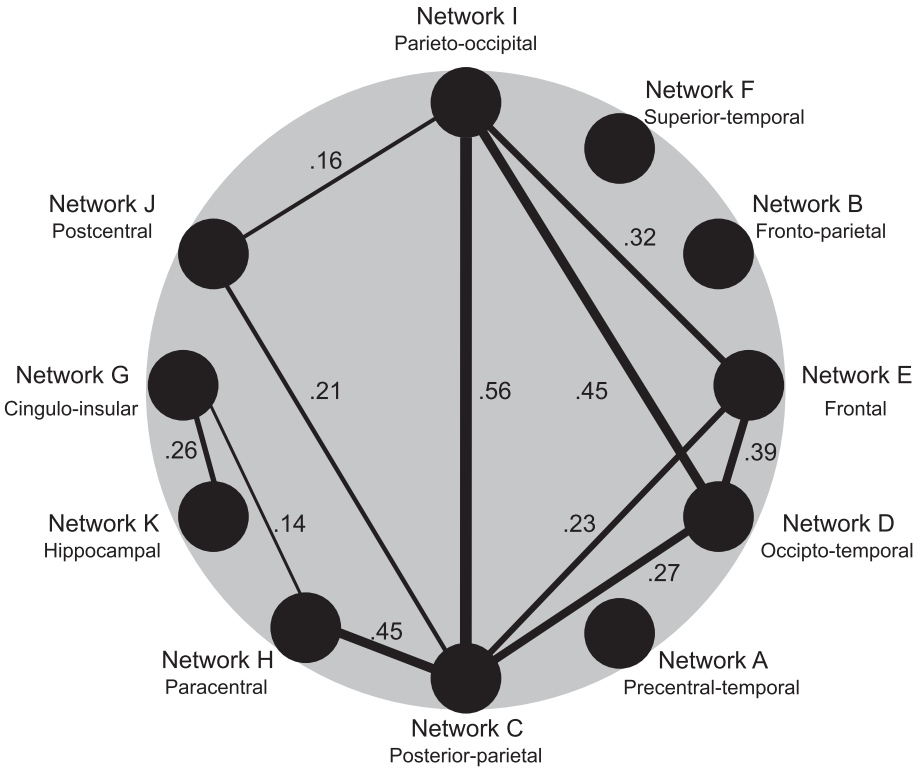

Fig. 3. Average functional network connectivity of macaque resting-state networks (RSNs). Lines and numerical values indicate functional connectivity between two RSNs in which there was a significant temporal correlation of their respective time-courses (one-sample Student *t*-test, $p<0.05$, corrected for multiple comparisons between 55 pairs, with a time lead/lag of $+/-3$ s). Network letters refer to spatial representations shown in Fig. 1.

current study revealed highly similar, possibly homologous macroscopic brain organization between macaques and humans. RSNs B (fronto-parietal), C (posterior-parietal), D (occipito-temporal), E (frontal), F (superior-temporal), H (paracentral), and I (parieto-occipital) have been commonly reported following ICA of human resting-state data (Beckmann et al., 2005; Jafri et al., 2008; Smith et al., 2009). These have been labeled oculomotor/dorsal attention (see Figs. 6g, h of Beckmann et al., 2005), default-mode (see Fig. 6e of Beckmann et al., 2005), higher-order visual (see Fig. 6b of Beckmann et al., 2005), executive (see Fig. 6f of Beckmann et al., 2005), auditory (see Fig. 6c of Beckmann et al., 2005), somatomotor (see Fig. 6d of Beckmann et al., 2005), and primary visual (see Fig. 6a of Beckmann et al., 2005) networks respectively. Further, RSNs G (cingulo-insular), J (postcentral), and K (hippocampal) though not consistently reported in studies utilizing ICA, have homologous networks that can be found when comparing task-based or seed-region analysis of human fMRI data (Kringelbach, 2005; Blatow et al., 2007; Burton et al., 2009; Vincent et al., 2006).

Two recent studies have examined resting-state connectivity with hypotheses derived from experimental anterograde tracer studies of the macaque monkey (Margulies et al., 2009; Kelly et al., 2010). Kelly et al. (2010) examined the connectivity of ventrolateral frontal areas with parietal and temporal cortex in the human cortex. They found that the human brain maintains the same basic patterns observed in nonhuman primates (Petrides and Pandya, 2009). In the same way, Margulies et al. (2009) found functional subdivisions of the precuneus to be preserved between both species and also consistent with tracer studies (Pandya and Seltzer, 1982). These findings suggest that resting-state functional connectivity reflects the underlying structural anatomy (discussed below) and taken together with our current results, support the role of the macaque as a suitable animal model in the study of human brain organization and cross-species comparisons of functional neuroanatomy.

Despite the strong similarities in many of the macaque RSNs to human RSNs, our study also revealed a number of notable differences in RSNs between the two species. There was an absence of two commonly reported, lateralized fronto-parietal RSNs implicated in cognitive attentional processes as well as memory and language functions (Beckmann et al., 2005; Jafri et al., 2008; Smith et al., 2009). The homologous macaque network, RSN B (frontoparietal), though encompassing the same brain regions as the human networks, was relatively symmetrical and did not suggest lateralization of function. Given that the macaque brain appears to be less lateralized than the human brain (Kagan et al., 2010), it is possible that the network represents the evolutionary predecessor to the lateralized human networks. Another functional connectivity difference was the lack of the dorsal medial prefrontal cortical (dmPFC) component of the DMN (Raichle et al., 2001). A relatively weak network connection has been previously reported (Vincent et al., 2010), though it was absent in two other studies (Vincent et al., 2007; Teichert et al., 2010). It is difficult to determine whether the dmPFC represents a less connected/weakly synchronized area of the DMN in the macaque, a brain area more vulnerable to BOLD fMRI artifactual sources (possibly due to the proximity to the eyes), an area highly sensitive to anesthesia level, or physiological variability in connectivity between animals. Finally, RSN K (hippocampal) shares a similar network pattern to the human memory RSN, however, there is an absence of parietal connectivity within the network that is found in the human brain (Vincent et al., 2006). RSN A (precentral–temporal) has not been reported as a separate network in resting-state or task-based studies of humans though the brain areas are implicated in more diffuse network patterns (Peeters et al., 2009). The ventral motor areas are critical for goal directed movements – particularly of the hand – in both species (Joly et al., 2009; Callaert et al., in press). In humans, however, there is a lateralization of motor function in which there is increased involvement of left motor areas resulting in functional asymmetries (Callaert et al., in press). Monkeys show a weaker motor dominance than humans (Leca et al., 2010) and the interhemispheric connectivity of the ventral motor system is supported by strong callosal connections between the homotopic functional areas. These factors could explain why a bilateral ventral motor RSN may not be found in the human at lower ICA model orders (20–40 ICs) as the synchronization between the systems might not be as tightly coupled.

RSNs are inferred from endogenous neural activity and their organization is likely shaped by structural connections (Sporns, 2010). There is increasing evidence to suggest that patterns of synchronous LFFs track underlying anatomical connectivity (Vincent et al., 2007; Hagmann et al., 2008; Skudlarski et al., 2008; Honey et al., 2009; Margulies et al., 2009; Kelly et al., 2010). Anatomical connectivity may underlie some of the RSNs that we identified in the present study. In some cases, the observed RSNs are in good agreement with the known major bundles of fibers that connect sensory association areas of posterior cortex to frontal cortex. RSN B (fronto-parietal) contains areas in frontal and parietal cortex that are connected by subcomponents II and III of the superior longitudinal fasciculus and RSN C (posterior-parietal) is comprised of areas that are connected by the fronto-occipital fasciculus (Petrides and Pandya, 2002b). Structural connectivity via the uncinate fasciculus may underlie RSN G (cingulo-insular) (Petrides and Pandya, 2002b). At least some of the areas in RSN D (occipito-temporal) are anatomically connected though the inferior longitudinal fasciculus (Petrides and Pandya, 2002b). Some of the other RSNs may reflect known connectivity by intrinsic connections (RSN E (Barbas and Pandya, 1989), RSN F (Pandya, 1995), RSN H (Vogt and Pandya, 1978)).

We also observed the opposite pattern in which little to no functional connectivity between hippocampal and parietal areas was observed whereas tracer methodology has revealed substantial connectivity between parietal and parahippocampal regions (Rockland and Van Hoesen, 1999). Similarly, RSN F (auditory) did not contain any prefrontal areas, despite the known connections of this area with ventral and dorsal areas through the extreme capsule (Petrides and Pandya, 2002b). It is important to note, however, the limitations of the data analysis when discussing the possible conclusions that are being drawn in terms of lateralization, connectivity, and absent homologous networks. Despite the link to structural organization, resting-state connectivity is not anatomical connectivity. The patterns of functional networks have been shown to capture polysynaptic connections (Vincent et al., 2007; O'Reilly et al., 2009) and functional connections have been shown where no direct structural connections exist (Uddin et al., 2008; Vincent et al., 2008; Honey et al., 2009). The discrepancies further highlight the need for an animal model as a method to constrain and interpret the false presence and absence of known connectivity in the human brain found using diffusion tensor imaging and resting-state methods. Only tracer studies can address direct connections and these are not typically feasible in human investigations.

A previous report examining changes in functional connectivity of the macaque during various visual stimulus contexts also examined two monkeys at rest under ketamine anesthesia using single-subject ICA (Moeller et al., 2009). Similar to the present study, networks encompassing primary sensory areas including auditory and visual systems were identified. These and other networks were typically bilateral, only comprising hemispheric functional homologous, a property also shown in rats (Hutchison et al., 2010). Our group data more closely resemble RSN organization of humans in which multiple subdivisions of a system are functionally connected. Functionally connected regions can split into separate components at higher model orders (Abou-Elseoud et al., 2010), a property that reflects the hierarchical functional organization of the brain (Cole et al., 2010). Moeller and colleagues used a model order of 300–1000 ICs whereas in the current study we used a model order of 20. The relatively large estimate could overestimate the number of networks and the use of

an automated sorting algorithm specifying bilateralism could bias the results towards those reported in the study.

To delineate the effects of single-subject ICA and model order, single-subject ICA was conducted on our same data set using a model order of 20. The individual component maps varied in their spatial correlation to the group RSNs within and between animals. The differences could reflect individual differences in morphology, structural connectivity, or functional connectivity as well as an exacerbation of weaker spatial dependencies causing the ICA to decompose the data differently. Variability could also arise from noise sources unique to each animal that were not extracted as a unique component using group-ICA. The results also highlighted intersubject variability in regards to network decomposition as often single subject networks comprised areas encompassed by two (or more) group RSNs. Overall, the individual networks had more diffuse functionally connectivity patterns than group-ICA and considerably more connectivity than the small-scale networks previously identified (Moeller et al., 2009). Therefore, the differences between our study and the work of Moeller et al. (2009) are more likely the result of a lower model order than group-level analysis. It is important to note however, that given the methodological differences including model order and anesthetic regime, a direct comparison between these studies is not possible.

Various network analysis strategies examining human and non-human primate brain connectivity have revealed that the cortex contains a small number of nodes having a disproportionately high number of connections (Sporns et al., 2007; Hagmann et al., 2008; Buckner et al., 2009). These highly connected nodes are referred to as hubs and serve to integrate diverse informational sources enabling globally efficient information flow (Sporns et al., 2007). Hubs also facilitate small-world network organization, minimizing wiring and metabolic costs by providing long-distance connections that integrate local networks (Bassett and Bullmore, 2006). The locations of high functional centrality have a close correspondence with structural hubs (Honey et al., 2007; Hagmann et al., 2008; Buckner et al., 2009). The present study revealed substantial inter-network functional connectivity with RSN C (posterior-parietal) and RSN I (parieto-occipital). The precuneous/posterior cingulate cortex areas encompassed by RSN C have been previously shown to possess both structural and functional hub properties in the human brain (Hagmann et al., 2008; Buckner et al., 2009) and could play a substantial role in integrating or regulating activity of other RSNs particularly at rest (Greicius et al., 2003). A detailed analysis of the structural connectivity of the macaque cortex based on tracer studies suggested several structural hubs including frontal area 46 and visual area V4 (Honey et al., 2007; Sporns et al., 2007) — areas encompassed by RSN I. These areas have been classified as association or integrative areas again reflecting their hub like properties. Thus, the results of the functional network connectivity analysis fit the current framework of known functional organization and further support the use of resting-state data in the evaluation of large-scale network dynamics and the use of FNC measures. It is important to note that like other functional connections, hubs have been shown to engage and disengage across time — dynamically altering their centrality (Honey et al., 2007). Evaluation of resting-state functional connectivity could provide an appropriate method to characterize the process by which the topology of functional networks changes over time.

Conclusions

In summary, our results demonstrate that ICA can identify RSNs in macaque monkeys that are likely homologous to those found in humans, thereby strongly supporting the use of monkeys as an ideal animal model for human brain function (Passingham, 2009) while also reinforcing the use of resting-state functional connectivity in delineating complex neural circuits in vivo.

Supplementary materials related to this article can be found online at doi:10.1016/j.neuroimage.2011.02.063.

Acknowledgments

This work was supported by a grant from the Canadian Institutes of Health Research (CIHR) to SE and a scholarship from the Natural Science and Engineering Research Council (NSERC) to RMH. We thank S. Hughes and B. Soper for technical assistance.

References

Abou-Elseoud, A., Starck, T., Remes, J., Nikkinen, J., Tervonen, O., Kiviniemi, V., 2010. The effect of model order selection in group PICA. Hum. Brain Mapp. 31, 1207–1216.
Auer, D.P., 2008. Spontaneous low-frequency blood oxygenation level-dependent fluctuations and functional connectivity analysis of the 'resting' brain. Magn. Reson. Imaging 26, 1055–1064.
Baker, J.T., Patel, G.H., Corbetta, M., Snyder, L.H., 2006. Distribution of activity across the monkey cerebral cortical surface, thalamus and midbrain during rapid, visually guided saccades. Cereb. Cortex 16, 447–459.
Barbas, H., Pandya, D.N., 1989. Architecture and intrinsic connections of the prefrontal cortex in the rhesus monkey. J. Comp. Neurol. 286, 353–375.
Bassett, D.S., Bullmore, E., 2006. Small-world brain networks. Neuroscientist 12, 512–523.
Beckmann, C.F., DeLuca, M., Devlin, J.T., Smith, S.M., 2005. Investigations into resting-state connectivity using independent component analysis. Philos. Trans. R. Soc. Lond. B Biol. Sci. 360, 1001–1013.
Biswal, B., Yetkin, F.Z., Haughton, V.M., Hyde, J.S., 1995. Functional connectivity in the motor cortex of resting human brain using echo-planar MRI. Magn. Reson. Med. 34, 537–541.
Blatow, M., Nennig, E., Durst, A., Sartor, K., Stippich, C., 2007. fMRI reflects functional connectivity of human somatosensory cortex. Neuroimage 37, 927–936.
Bruce, C.J., Goldberg, M.E., 1985. Primate frontal eye fields. I. Single neurons discharging before saccades. J. Neurophysiol. 53, 603–635.
Buckner, R.L., Sepulcre, J., Talukdar, T., Krienen, F.M., Liu, H., Hedden, T., Andrews-Hanna, J.R., Sperling, R.A., Johnson, K.A., 2009. Cortical hubs revealed by intrinsic functional connectivity: mapping, assessment of stability, and relation to Alzheimer's disease. J. Neurosci. 29, 1860–1873.
Burton, H., Dixit, S., Litkowski, P., Wingert, J.R., 2009. Functional connectivity for somatosensory and motor cortex in spastic diplegia. Somatosens. Mot. Res. 26, 90–104.
Buxhoeveden, D.P., Switala, A.E., Roy, E., Litaker, M., Casanova, M.F., 2001. Morphological differences between minicolumns in human and nonhuman primate cortex. Am. J. Phys. Anthropol. 115, 361–371.
Calhoun, V.D., Adali, T., Pearlson, G.D., Pekar, J.J., 2001. A method for making group inferences from functional MRI data using independent component analysis. Hum. Brain Mapp. 14, 140–151.
Calhoun, V.D., Adali, T., Pekar, J.J., Pearlson, G.D., 2003. Latency (in) sensitive ICA: group independent component analysis of fMRI data in the temporal frequency domain. Neuroimage 20, 1661–1669.
Callaert, D.V., Vercauteren, K., Peeters, R., Tam, F., Graham, S., Swinnen, S.P., Sunaert, S., Wenderoth, N., in press. Hemispheric asymmetries of motor versus nonmotor processes during (visuo)motor control. Hum. Brain. Mapp.
Cole, D.M., Smith, S.M., Beckmann, C.F., 2010. Advances and pitfalls in the analysis and interpretation of resting-state FMRI data. Front. Syst. Neurosci. 4, 8.
Cordes, D., Haughton, V.M., Arfanakis, K., Wendt, G.J., Turski, P.A., Moritz, C.H., Quigley, M.A., Meyerand, M.E., 2000. Mapping functionally related regions of brain with functional connectivity MR imaging. Am. J. Neuroradiol. 21, 1636–1644.
Croxson, P.L., Johansen-Berg, H., Behrens, T.E., Robson, M.D., Pinsk, M.A., Gross, C.G., Richter, W., Richter, M.C., Kastner, S., Rushworth, M.F., 2005. Quantitative investigation of connections of the prefrontal cortex in the human and macaque using probabilistic diffusion tractography. J. Neurosci. 25, 8854–8866.
Damoiseaux, J.S., Rombouts, S.A., Barkhof, F., Scheltens, P., Stam, C.J., Smith, S.M., Beckmann, C.F., 2006. Consistent resting-state networks across healthy subjects. Proc. Natl. Acad. Sci. U.S.A. 103, 13848–13853.
Demirci, O., Stevens, M.C., Andreasen, N.C., Michael, A., Liu, J., White, T., Pearlson, G.D., Clark, V.P., Calhoun, V.D., 2009. Investigation of relationships between fMRI brain networks in the spectral domain using ICA and Granger causality reveals distinct differences between schizophrenia patients and healthy controls. Neuroimage 46, 419–431.
Dum, R.P., Strick, P.L., 2002. Motor areas in the frontal lobe of the primate. Physiol. Behav. 77, 677–682.
Farber, N.E., Harkin, C.P., Niedfeldt, J., Hudetz, A.G., Kampine, J.P., Schmeling, W.T., 1997. Region-specific and agent-specific dilation of intracerebral microvessels by volatile anesthetics in rat brain slices. Anesthesiology 87, 1191–1198.
Felleman, D.J., Van Essen, D.C., 1991. Distributed hierarchical processing in the primate cerebral cortex. Cereb. Cortex 1, 1–47.
Ford, K.A., Gati, J.S., Menon, R.S., Everling, S., 2009. BOLD fMRI activation for anti-saccades in nonhuman primates. Neuroimage 45, 470–476.
Fox, M.D., Raichle, M.E., 2007. Spontaneous fluctuations in brain activity observed with functional magnetic resonance imaging. Nat. Rev. Neurosci. 8, 700–711.
Friston, K.J., 1994. Functional and effective connectivity in neuroimaging: a synthesis. Hum. Brain Mapp. 2, 56–78.

Friston, K.J., 2002. Beyond phrenology: what can neuroimaging tell us about distributed circuitry. Annu. Rev. Neurosci. 25, 221–250.
Greicius, M., 2008. Resting-state functional connectivity in neuropsychiatric disorders. Curr. Opin. Neurol. 21, 424–430.
Greicius, M.D., Krasnow, B., Reiss, A.L., Menon, V., 2003. Functional connectivity in the resting brain: a network analysis of the default mode hypothesis. Proc. Natl. Acad. Sci. U.S.A. 100, 253–258.
Greicius, M.D., Supekar, K., Menon, V., Dougherty, R.F., 2009. Resting-state functional connectivity reflects structural connectivity in the default mode network. Cereb. Cortex 19, 72–78.
Guye, M., Bartolomei, F., Ranjeva, J.P., 2008. Imaging structural and functional connectivity: towards a unified definition of human brain organization? Curr. Opin. Neurol. 21, 393–403.
Hagmann, P., Cammoun, L., Gigandet, X., Meuli, R., Honey, C.J., Wedeen, V.J., Sporns, O., 2008. Mapping the structural core of human cerebral cortex. PLoS Biol. 6, e159.
Hampson, M., Peterson, B.S., Skudlarski, P., Gatenby, J.C., Gore, J.C., 2002. Detection of functional connectivity using temporal correlations in MR images. Hum. Brain Mapp. 15, 247–262.
Himberg, J., Hyvarinen, A., Esposito, F., 2004. Validating the independent components of neuroimaging time series via clustering and visualization. Neuroimage 22, 1214–1222.
Honey, C.J., Kötter, R., Breakspear, M., Sporns, O., 2007. Network structure of cerebral cortex shapes functional connectivity on multiple time scales. Proc. Natl. Acad. Sci. U.S.A. 104, 10240–10245.
Honey, C.J., Sporns, O., Cammoun, L., Gigandet, X., Thiran, J.P., Meuli, R., Hagmann, P., 2009. Predicting human resting-state functional connectivity from structural connectivity. Proc. Natl. Acad. Sci. U.S.A. 106, 2035–2040.
Hutchison, R.M., Mirsattari, S.M., Jones, C.K., Gati, J.S., Leung, L.S., 2010. Functional networks in the anesthetized rat brain revealed by independent component analysis of resting-state fMRI. J. Neurophysiol. 103, 3398–3406.
Jafri, M.J., Pearlson, G.D., Stevens, M., Calhoun, V.D., 2008. A method for functional network connectivity among spatially independent resting-state components in schizophrenia. Neuroimage 39, 1666–1681.
Johnston, K., Everling, S., 2008. Neurophysiology and neuroanatomy of reflexive and voluntary saccades in non-human primates. Brain Cogn. 68, 271–283.
Joly, O., Vanduffel, W., Orban, G.A., 2009. The monkey ventral premotor cortex processes 3D shape from disparity. Neuroimage 47, 262–272.
Kaas, J.H., 1993. The functional organization of somatosensory cortex in primates. Ann. Anat. 175, 509–518.
Kagan, I., Iyer, A., Lindner, A., Andersen, R.A., 2010. Space representation for eye movements is more contralateral in monkeys than in humans. Proc. Natl. Acad. Sci. U.S.A. 107, 7933–7938.
Kelly, C., Uddin, L.Q., Shehzad, Z., Margulies, D.S., Castellanos, F.X., Milham, M.P., Petrides, M., 2010. Broca's region: linking human brain functional connectivity data and non-human primate tracing anatomy studies. Eur. J. Neurosci. 32, 383–398.
Kiviniemi, V.J., Haanpää, H., Kantola, J.H., Jauhiainen, J., Vainionpää, V., Alahuhta, S., Tervonen, O., 2005. Midazolam sedation increases fluctuation and synchrony of the resting brain BOLD signal. Magn. Reson. Imaging 23, 531–537.
Koyama, M., Hasegawa, I., Osada, T., Adachi, Y., Nakahara, K., Miyashita, Y., 2004. Functional magnetic resonance imaging of macaque monkeys performing visually guided saccade tasks: comparison of cortical eye fields with humans. Neuron 41, 795–807.
Kringelbach, M.L., 2005. The human orbitofrontal cortex: linking reward to hedonic experience. Nat. Rev. Neurosci. 6, 691–702.
Leca, J.B., Gunst, N., Huffman, M.A., 2010. Principles and levels of laterality in unimanual and bimanual stone handling patterns by Japanese macaques. J. Hum. Evol. 58, 155–165.
Li, Y.O., Adali, T., Calhoun, V.D., 2007. Estimating the number of independent components for functional magnetic resonance imaging data. Hum. Brain Mapp. 28, 1251–1266.
Liao, R., McKeown, M.J., Krolik, J.L., 2006. Isolation and minimization of head motion-induced signal variations in fMRI data using independent component analysis. Magn. Reson. Med. 55, 1396–1413.
Margulies, D.S., Vincent, J.L., Kelly, C., Lohmann, G., Uddin, L.Q., Biswal, B.B., Villringer, A., Castellanos, F.X., Milham, M.P., Petrides, M., 2009. Precuneus shares intrinsic functional architecture in humans and monkeys. Proc. Natl. Acad. Sci. U.S.A. 106, 20069–20074.
Miller, E.K., Cohen, J.D., 2001. An integrative theory of prefrontal cortex function. Annu. Rev. Neurosci. 24, 167–202.
Moeller, S., Nallasamy, N., Tsao, D.Y., Freiwald, W.A., 2009. Functional connectivity of the macaque brain across stimulus and arousal states. J. Neurosci. 29, 5897–5909.
Nakahara, K., Adachi, Y., Osada, T., Miyashita, Y., 2007. Exploring the neural basis of cognition: multi-modal links between human fMRI and macaque neurophysiology. Trends Cogn. Sci. 11, 84–92.
Nelissen, K., Luppino, G., Vanduffel, W., Rizzolatti, G., Orban, G.A., 2005. Observing others: multiple action representation in the frontal lobe. Science 310, 332–336.
Noudoost, B., Chang, M.H., Steinmetz, N.A., Moore, T., 2010. Top-down control of visual attention. Curr. Opin. Neurobiol. 20, 183–190.
O'Reilly, J.X., Beckmann, C.F., Tomassini, V., Ramnani, N., Johansen-Berg, H., 2009. Distinct and overlapping functional zones in the cerebellum defined by resting state functional connectivity. Cereb. Cortex 20, 953–965.
Ongür, D., Ferry, A.T., Price, J.L., 2003. Architectonic subdivision of the human orbital and medial prefrontal cortex. J. Comp. Neurol. 460, 425–449.
Orban, G.A., Van Essen, D., Vanduffel, W., 2004. Comparative mapping of higher visual areas in monkeys and humans. Trends Cogn. Sci. 8, 315–324.
Pandya, D.N., 1995. Anatomy of the auditory cortex. Rev. Neurol. (Paris) 151, 486–494.
Pandya, D.N., Seltzer, B., 1982. Intrinsic connections and architectonics of posterior parietal cortex in the rhesus monkey. J. Comp. Neurol. 204, 196–210.
Passingham, R., 2009. How good is the macaque monkey model of the human brain? Curr. Opin. Neurobiol. 19, 6–11.
Peeters, R., Simone, L., Nelissen, K., Fabbri-Destro, M., Vanduffel, W., Rizzolatti, G., Orban, G.A., 2009. The representation of tool use in humans and monkeys: common and uniquely human features. J. Neurosci. 29, 11523–11539.
Perlbarg, V., Bellec, P., Anton, J.L., Pélégrini-Issac, M., Doyon, J., Benali, H., 2007. CORSICA: correction of structured noise in fMRI by automatic identification of ICA components. Magn. Reson. Imaging 25, 35–46.
Petkov, C.I., Kayser, C., Steudel, T., Whittingstall, K., Augath, M., Logothetis, N.K., 2008. A voice region in the monkey brain. Nat. Neurosci. 11, 367–374.
Petrides, M., Pandya, D.N., 1999. Dorsolateral prefrontal cortex: comparative cytoarchitectonic analysis in the human and the macaque brain and corticocortical connection patterns. Eur. J. Neurosci. 11, 1011–1036.
Petrides, M., Pandya, D.N., 2002a. Comparative cytoarchitectonic analysis of the human and the macaque ventrolateral prefrontal cortex and corticocortical connection patterns in the monkey. Eur. J. Neurosci. 16, 291–310.
Petrides, M., Pandya, D.N., 2002b. Association pathways of the prefrontal cortex and functional observations. In: Stuss, D.T., Knight, R.T. (Eds.), Principles of Frontal Lobe Function. Oxford University Press, New York, NY, pp. 31–84.
Petrides, M., Pandya, D.N., 2009. Distinct parietal and temporal pathways to the homologues of Broca's area in the monkey. PLoS Biol. 7, e1000170.
Petrides, M., Cadoret, G., Mackey, S., 2005. Orofacial somatomotor responses in the macaque monkey homologue of Broca's area. Nature 435, 1235–1238.
Phillips, C.G., Porter, R., 1977. Corticospinal Neurons. Academic Press, London.
Preuss, T.M., 2000. Taking the measure of diversity: comparative alternatives to the model-animal paradigm in cortical neuroscience. Brain Behav. Evol. 55, 287–329.
Preuss, T.M., 2004. Specializations of the human visual system: the monkey model meets human reality. In: Kaas, J.H., Collins, C.E. (Eds.), The Primate Visual System. CRC Press, pp. 231–259.
Raichle, M.E., MacLeod, A.M., Snyder, A.Z., Powers, W.J., Gusnard, D.A., Shulman, G.L., 2001. A default mode of brain function. Proc. Natl. Acad. Sci. U.S.A. 98, 676–682.
Rauschecker, J.P., Scott, S.K., 2009. Maps and streams in the auditory cortex: nonhuman primates illustrate human speech processing. Nat. Neurosci. 12, 718–724.
Rees, G., Friston, K., Koch, C., 2000. A direct quantitative relationship between the functional properties of human and macaque V5. Nat. Neurosci. 3, 716–723.
Rilling, J., 2006. Human and nonhuman primate brains: are they allometrically scaled versions of the same design? Evol. Anthropol. 15, 65–77.
Rockland, K.S., Van Hoesen, G.W., 1999. Some temporal and parietal cortical connections converge in CA1 of the primate hippocampus. Cereb. Cortex 9, 232–237.
Rolls, E.T., Cahusac, P.M., Feigenbaum, J.D., Miyashita, Y., 1993. Responses of single neurons in the hippocampus of the macaque related to recognition memory. Exp. Brain Res. 93, 299–306.
Schlag, J., Schlag-Rey, M., 1987. Evidence for a supplementary eye field. J. Neurophysiol. 57, 179–200.
Shmuel, A., Leopold, D.A., 2008. Neuronal correlates of spontaneous fluctuations in fMRI signals in monkey visual cortex: implications for functional connectivity at rest. Hum. Brain Mapp. 29, 751–761.
Skudlarski, P., Jagannathan, K., Calhoun, V.D., Hampson, M., Skudlarska, B.A., Pearlson, G., 2008. Measuring brain connectivity: diffusion tensor imaging validates resting state temporal correlations. Neuroimage 43, 554–561.
Smith, S.M., Fox, P.T., Miller, K.L., Glahn, D.C., Fox, P.M., Mackay, C.E., Filippini, N., Watkins, K.E., Toro, R., Laird, A.R., Beckmann, C.F., 2009. Correspondence of the brain's functional architecture during activation and rest. Proc. Natl. Acad. Sci. U.S.A. 106, 13040–13045.
Sporns, O., 2010. Networks of the Brain. MIT Press, Cambridge.
Sporns, O., Tononi, G., Kötter, R., 2005. The human connectome: a structural description of the human brain. PLoS Comput. Biol. 1, 245–251.
Sporns, O., Honey, C.J., Kötter, R., 2007. Identification and classification of hubs in brain networks. PLoS ONE 2, e1049.
Squire, L.R., Zola-Morgan, S., 1991. The medial temporal lobe memory system. Science 253, 1380–1386.
Stefanacci, L., Reber, P., Constanza, J., Wong, E., Buxton, R., Zola, S., Squire, L., Albright, T., 1998. fMRI of monkey visual cortex. Neuron 20, 1051–1057.
Teichert, T., Grinband, J., Hirsch, J., Ferrera, V.P., 2010. Effects of heartbeat and respiration on macaque fMRI: implications for functional connectivity. Neuropsychologia 48, 1886–1894.
Thomas, C.G., Harshman, R.A., Menon, R.S., 2002. Noise reduction in BOLD-based fMRI using component analysis. Neuroimage 17, 1521–1537.
Tsao, D.Y., Freiwald, W.A., Knutsen, T.A., Mandeville, J.B., Tootell, R.B., 2003. Faces and objects in macaque cerebral cortex. Nat. Neurosci. 6, 989–995.
Uddin, L.Q., Mooshagian, E., Zaidel, E., Scheres, A., Margulies, D.S., Kelly, A.M., Shehzad, Z., Adelstein, J.S., Castellanos, F.X., Biswal, B.B., Milham, M.P., 2008. Residual functional connectivity in the split-brain revealed with resting-state functional MRI. NeuroReport 19, 703–709.
Van Essen, D.C., 2004. Surface-based approaches to spatial localization and registration in primate cerebral cortex. Neuroimage 23 (Suppl 1), S97–S107.
Vincent, J.L., Snyder, A.Z., Fox, M.D., Shannon, B.J., Andrews, J.R., Raichle, M.E., Buckner, R.L., 2006. Coherent spontaneous activity identifies a hippocampal–parietal memory network. J. Neurophysiol. 96, 3517–3531.

Vincent, J.L., Patel, G.H., Fox, M.D., Snyder, A.Z., Baker, J.T., Van Essen, D.C., Zempel, J.M., Snyder, L.H., Corbetta, M., Raichle, M.E., 2007. Intrinsic functional architecture in the anaesthetized monkey brain. Nature 447, 83–86.

Vincent, J.L., Kahn, I., Snyder, A.Z., Raichle, M.E., Buckner, R.L., 2008. Evidence for a frontoparietal control system revealed by intrinsic functional connectivity. J. Neurophysiol. 100, 3328–3342.

Vincent, J.L., Kahn, I., Van Essen, D.C., Buckner, R.L., 2010. Functional connectivity of the macaque posterior parahippocampal cortex. J. Neurophysiol. 103, 793–800.

Vogt, B.A., Pandya, D.N., 1978. Cortico-cortical connections of somatic sensory cortex (areas 3, 1, and 2) in the rhesus money. J. Comp. Neurol. 177, 179–192.

Wirth, S., Yanike, M., Frank, L.M., Smith, A.C., Brown, E.N., Suzuki, W.A., 2003. Single neurons in the monkey hippocampus and learning of new associations. Science 300, 1578–1581.

Young, M.P., 1993. The organization of neural systems in the primate cerebral cortex. Proc. R. Soc. Lond. B 252, 13–18.